Available online at www.sciencedirect.com
ScienceDirect
Catalysis Today 133–135 (2008) 428–434
CATALYSIS TODAY
www.elsevier.com/locate/cattod

The inhibiting effect of extra-framework Al on monolithic Co-ZSM5 catalysts used for NO_x SCR

A.V. Boix [a,*], E.E. Miró [a], E.A. Lombardo [a], J.L.G. Fierro [b]

[a] *Instituto de Investigaciones en Catálisis y Petroquímica – INCAPE (FIQ,UNL-CONICET), Santiago del Estero 2829, 3000 Santa Fe, Argentina*
[b] *Instituto de Catálisis y Petroleoquímica – CSIC, c/Marie Curie 2, Cantoblanco UAM, 28049, Madrid, Spain*

Available online 1 February 2008

Abstract

Co-zeolite catalysts are active for the NO_x selective reduction with CH_4. For practical purposes, they should be in the form of monoliths and a binder should be added to firmly attach the Co-zeolite powders to the monoliths. The incorporation of $Al(NO_3)_3$ as a binder to the Co-ZSM5/cordierite monolith system led to a sharp decrease of the N_2 selectivity compared to the original Co-ZSM5 powder. A systematic study was conducted to identify the species formed during the preparation of samples obtained by either ionic exchange or impregnation of the cobalt acetate using different supports (Na-ZSM5, H-ZSM5, and SiO_2) and co-impregnating $Al(NO_3)_3$ in varying proportions. It was found that the simultaneous presence of Al^{3+} and Co^{2+} in washcoating suspension led to a strong interaction that impaired the incorporation of the latter to the zeolite exchange sites, generating a new $Co_{1+y}Al_{2-x}O_4$ species after calcining the solid at 550 °C. The Raman spectra of impregnated samples showed the band at 755–770 cm^{-1} characteristic of the $CoAl_2O_4$ spinel together with the other lines (690, 619, 523 and 482 cm^{-1}), which coincided with those of Co_3O_4. The modified Auger parameter revealed the presence of octahedrally coordinated Al^{3+} when SiO_2 was the support. This was also consistent with the appearance of the XRD reflections of Co_2AlO_4 and $CoAl_2O_4$. The Raman spectrum of Co-exchanged samples plus Al^{3+} added in the slurry showed a strong band at 595 cm^{-1} corresponding to Co_xO_y. The band at 690 cm^{-1} was weak indicating that the Co_3O_4 and $CoAl_2O_4$ phases were not well developed. These results, together with the TPR patterns support the hypothesis that a $Co_{1+y}Al_{2-x}O_4$ non-stoichiometric spinel is responsible for its poor activity in the NO_x SCR with methane.

Keywords: Binder catalytic effect; Methane reductant; Cobalt aluminate

1. Introduction

The catalysts used for pollution control in combustion exhausts must be shaped as monoliths in order to be suitable for high-flow rates and dusty gases. Washcoating on cordierite monoliths is the most widely employed procedure for attaching the active phases on the monolith walls. Abundant information is available even in the open literature concerning the washcoating of alumina, the material used in commercial three-way catalysts [1].

Adhesion of the washcoat to the monolith walls is a critical factor since the loss of the catalyst via attrition or erosion is a serious source of irreversible deactivation. To improve the coating adherence, a binder is usually employed, consisting of different oxides (alumina, silica) or their precursors such as metal nitrates [2]. Among them, alumina is probably the most frequently used. The function of these oxides is to provide a bind between the catalyst particles and the monolith by increasing the points of contact between particles and that of the particles with the monolith walls [3]. However, in certain cases, the binder particles may affect the catalytic behavior. Our group has recently prepared a PtCo ferrierite-washcoated cordierite monolith adding SiO_2 as a binder. This formulation resulted in an active and thermally stable catalyst for the SCR of NO with CH_4 in the presence of water [4]. On the other hand, in a recent publication [5] we showed that $Al(NO_3)_3$ used as a binder produced undesirable changes in the catalytic behavior, suggesting that this effect is due to the formation of a non-stoichiometric cobalt aluminate during the calcination of the monolith at 550 °C.

Co-zeolite systems are complex due to the different Co-species that can be formed. For example, after calcination the

* Corresponding author.
E-mail address: aboix@fiqus.unl.edu.ar (A.V. Boix).

0920-5861/$ – see front matter © 2007 Elsevier B.V. All rights reserved.
doi:10.1016/j.cattod.2007.12.122

Co-ZSM5 catalyst contains Co_3O_4, Co^{2+} located at exchange positions and non-crystalline oxo-species [5]. Even more complex systems can be generated with the addition of another cation (as a noble metal) or aluminum (binder), as in the present work. When platinum is exchanged together with Co in a ZSM5, the location of the Co^{2+} ion changes [5], a large fraction migrates to internal lattice positions. In used catalysts, Co_3O_4 is formed in Co-ZSM5, but in PtCo-ZSM5 highly dispersed non-crystalline Co species are found in the zeolitic matrix [2]. As mentioned above, a non-stoichiometric cobalt aluminate is likely to be formed when extra-lattice Al is present. Under reaction conditions, the $Co_{1+y}Al_{2-x}O_4$ spinel may partially decompose to yield Co_3O_4, thus increasing combustion activity and decreasing the selectivity for the NO_x to N_2 reaction, which is the desired one.

The aim of this work is to gain insight into the effect of Al–Co interactions on the different Co species formed inside the ZSM5 framework. These interactions can take place not only when Al-containing binders are used for Co-zeolite washcoating but also when extra-framework Al is generated during zeolite dealumination occurring under reaction conditions. To this end, a systematic series of experiments was set up. Catalysts were prepared with various Al/Co ratios, Co being either exchanged or impregnated in ZSM5 and SiO_2, the last support used as reference. The samples were thoroughly characterized by X-ray diffraction (XRD), X-ray photoelectron spectroscopy (XPS), laser Raman spectroscopy (LRS) and temperature-programmed reduction (TPR).

2. Experimental

2.1. Preparation of the different solids

2.1.1. Co-exchanged Na-ZSM5 and NH_4-ZSM5

Catalysts were prepared by ionic exchange starting from NH_4-ZSM5 (Zeolyst, atomic ratio, Si/Al = 15) and Na-ZSM5 (Linde, Si/Al = 9.6). Co-exchanged ZSM5 solids were prepared using cobalt acetate solution (0.025 M), with 5 g/L (zeolite/solution) ratio. The exchange time was 24 h at 80 °C and then the solids were filtered, washed and dried at 120 °C for 2 h. Co-ZSM5 was calcined, heating at 2 °C/min in O_2 flow up to 400 °C. The chemical composition of the two catalysts was 3.7 and 4.9 wt% of Co on NH_4-ZSM5 ($Co_{3.7}Z$) and Na-ZSM5 ($Co_{4.9}Z$), respectively. These cobalt contents corresponding to (Co^{2+}/Al) atomic ratio of 0.65 and 0.57, respectively.

2.1.2. Co-ZSM5 + $Al(NO_3)_3$ washcoat

The sample was prepared by adding 2 wt% aluminum nitrate to the Co-ZSM5 (4.9 wt% Co) aqueous suspension (ratio Al_{ad}/Co = 0.5), denoted $Co_{4.9}Z + Al(NO_3)_3$. Then, it was dried at 120 °C for 12 h and afterwards calcined in oxygen flow at 550 °C for 2 h.

2.1.3. The modified washcoat

An aqueous suspension was prepared by adding aluminum nitrate and Na-ZSM5 to a cobalt acetate solution in proportions similar to the original washcoat. It was dried and calcined in oxygen flow at two different temperatures, 400 or 550 °C, for 2 h.

2.1.4. Al-Co-/H-ZSM5 and Al-Co/SiO_2

Two series of samples were obtained by incipient-wetness impregnation of 2 g of either H-ZSM5 (350 m^2/g) or SiO_2 (20 m^2/g) with an aqueous cobalt acetate and aluminum nitrate solution. All the samples contained 4.5 wt% of cobalt and variable Al_{ad}/Co ratios: 0.15, 0.30, 0.90, 1.50 and were calcined in oxygen flow at 550 °C for 2 h.

2.2. Catalytic measurements

The powdered and monolithic catalysts were evaluated in a continuous flow system. The typical composition of the reactant feedstream was the following: 1000 ppm NO, 1000 ppm CH_4, 2% O_2 in helium. The reaction was performed under atmospheric pressure between 250 and 650 °C, with Gas-hourly space velocity, GHSV = 10,000 h^{-1} (flow × density of the zeolite/zeolite mass). The washcoated monoliths (1 cm × 1 cm × 2 cm) were placed in the same reactor between two quartz wool plugs, and the quartz tube was filled with CSi particles to avoid bypass flow. The GHSV = flow rate × zeolite apparent density/zeolite mass was calculated on the basis of the mass of the zeolite loaded in the monolith. In this way, catalytic results obtained with washcoated monoliths can be compared with those of the powder zeolites.

The gaseous mixtures were analyzed with an SRI 9300B chromatograph equipped with two columns, a 5 Å molecular sieve and a Chromosorb 102. The NO_x conversion (C_{N_2}) was calculated from N_2 production, like $C_{N_2} = 2 \times 100([N_2]/[NO]^0)$, where $[NO]^0$ is the feed NO concentration.

The CH_4 conversion (C_{CH_4}) was calculated as $C_{CH_4} = 100([CH_4]^0 - [CH_4])/[CH_4]^0$.

2.3. Catalysts characterization

2.3.1. TPR experiments

They were performed using an Okhura TP-2002S instrument equipped with a TCD detector. The reducing gas was 5% H_2 in Ar, flowing at 30 mL/min and the heating rate was 10 K/min up to 900 °C. 0.050 g fresh powder samples, were pre-treated in situ with O_2 flow prior to the experiment.

2.3.2. Raman spectroscopy

The Raman spectra were recorded with a TRS-600-SZ-P Jasco Laser Raman instrument, equipped with a CCD (charge-coupled device) with the detector cooled to about 153 K using liquid N_2. The excitation source was the 514.5 nm line of a Spectra 9000 Photometrics Ar ion laser. The laser power was set at 30 mW. For these measurements, the calcined powder samples were pressed at 4 bar into self-supporting wafers.

2.3.3. X-ray photoelectron spectroscopy

X-ray photoelectron spectra were acquired with an ESCALAB 200R electron spectrometer equipped with a hemispherical electron analyzer and AlK_α X-ray source

($h\nu$ = 1486.6 eV). The Si2p, Al2p, Co2p, O1s and C1s core-level spectra and kinetic energy of the $Al_{(KLL)}$ Auger peak were recorded. The modified Auger parameter (α') of aluminum was calculated by the following equation:

$$\alpha' = \text{BE Al2p} + \text{KE Al}_{(KLL)}$$

where BE Al2p is the binding energy of the Al2p XPS peak and KE $Al_{(KLL)}$ is the kinetic energy of the Al (KL_{23} L_{23}) Auger transition.

2.3.4. X-Ray diffraction (XRD)

The XRD patterns of the calcined and used solids were obtained with an XD-D1 Shimadzu instrument, using CuKα radiation at 35 kV and 40 mA. The scan rate was 1°/min for 2θ values between 5° and 80°.

3. Results and discussion

3.1. Catalytic behavior

Fig. 1 shows the catalytic performance of $Co_{4.9}$ZSM-5, both as a powder and washcoated on a cordierite monolith without added binder. Its ability to reduce NO_x to NO was about the same with maxima located at ca. 450–500 °C. On the other hand, when $Al(NO_3)_3$ was added as a binder to improve adherence, the NO_x conversion sharply dropped below 5% conversion. Note that the methane oxidation was slightly affected in the case of the powder catalyst and remained essentially the same when monoliths were used. The same effects were observed with other ZSM5 materials of varying origins, different Si/Al ratios and cobalt concentrations [5]. In what follows, we will try to provide experimental evidence to understand the deleterious effect of the $Al(NO_3)_3$ binder upon the SCR of NO_x.

3.2. Temperature-programmed reduction (TPR) results

TPR experiments were performed to obtain information about cobalt species and their distribution in the zeolite matrix. Fig. 2A and Table 1 show results obtained with Co-exchanged NH_4 and Na-ZSM5, as reference samples. Both of them present two reduction zones with a maximum centered at 263 and 665 °C for $Co_{3,7}$-ZSM5 (Si/Al = 15) which was obtained from NH_4-ZSM5 as starting material and in 450 and 710 °C for $Co_{4.9}$-ZSM5 (Si/Al = 10), obtained from Na-ZSM5. In spite of the high Co content achieved during ion exchange more than 85% of the metal is located at exchange positions, the remaining fraction being segregated oxides (CoO and Co_3O_4). As seen in Table 1, while for $Co_{3.7}$-ZSM5 80% of the Co^{2+} ions are reduced at 665 °C, for $Co_{4.9}$-ZSM5 only 40% are indicating that in the latter case Co^{2+} ions are better stabilized in the zeolite framework.

In order to study the interaction between exchanged Co species and the $Al(NO_3)_3$ added as a binder during the washcoating procedure, two types of samples were prepared: (i) $Co_{4.9}$Z + Al, where the $Al(NO_3)_3$ was dissolved in a slurry of CoNaZSM5 and (ii) the slurry was prepared from NaZSM5, cobalt acetate and aluminum nitrate. The latter preparation was calcined at 400 °C and a fraction at 550 °C. The first temperature value was the one commonly used when powders are prepared, and the higher value was used for calcination of washcoated monoliths.

Fig. 2B shows reduction profiles of different preparations obtained in the presence of $Al(NO_3)_3$. The $Co_{4.9}$Z + Al sample has only one reduction peak centered at 580 °C, where 94% of the Co is reduced. When the slurry is prepared from the salts (method ii), the profiles also show a single major peak, but at lower temperatures, 490 °C for the sample calcined at 400 °C and 512 °C for that calcined at 550 °C, with a H_2/Co ratio of 0.9 and 1.09, respectively.

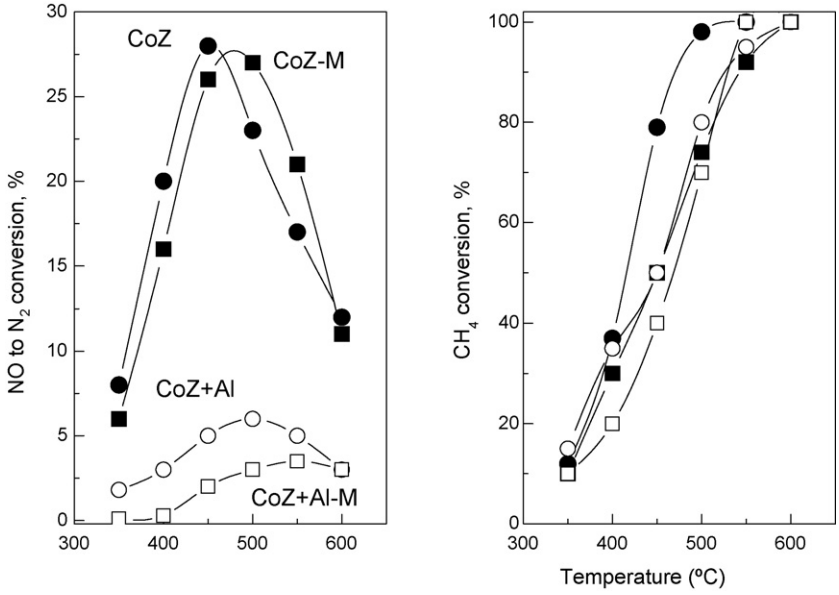

Fig. 1. Catalytic behavior in the SCR of NO with CH_4. Reaction conditions: 1000 ppm NO, 1000 ppm CH_4, 2% O_2 in He, GHSV = 10,000 h^{-1}. (●) $Co_{4.9}$Z powder; (■) $Co_{4.9}$Z washcoated monolith; (○) $Co_{4.9}$Z + $Al(NO_3)_3$ powder (Al_{ad}/Co = 0.5); (□) $Co_{4.9}$Z + Al washcoated monolith.

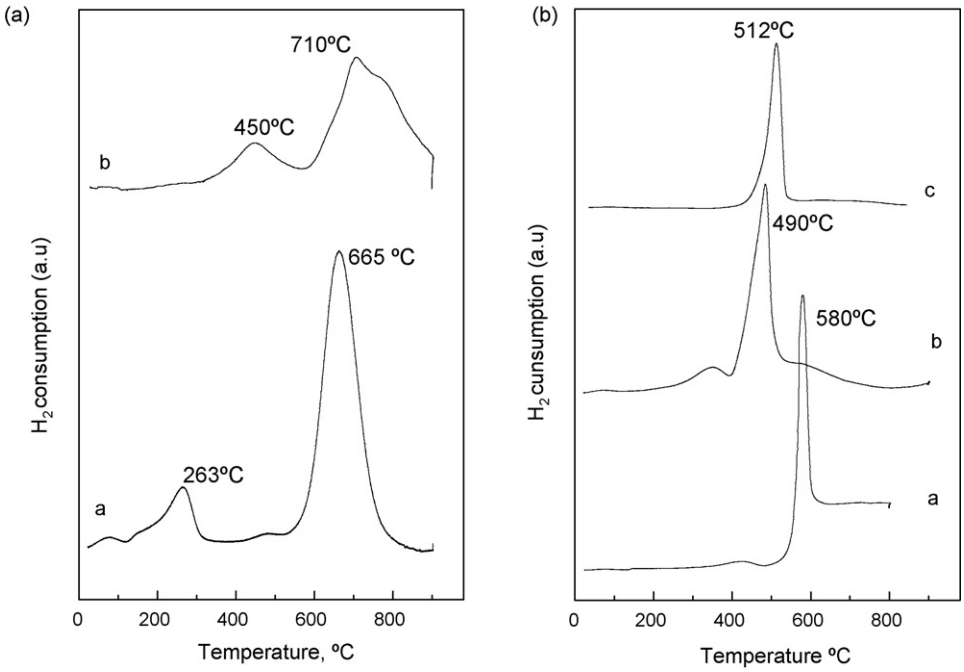

Fig. 2. (A) TPR of Co-exchanged Na- and NH_4-ZSM5: (a) $Co_{3.7}Z$; (b) $Co_{4.9}Z$, both calcined in situ at 400 °C. (B) TPR of CoZ plus $Al(NO_3)_3$ washcoating precursors. (a) $Co_{4.9}Z$ + Al; (b) Al-Co + NaZ calcined at 400 °C and (c) Al-Co + NaZ calcined at 550 °C.

Comparing Fig. 2A and B, it is observed that the Co species formed when Al is present are reduced at temperatures higher than that of cobalt oxides (usually in the 250–350 °C range) but lower than those required for reducing Co^{2+} ions at exchange sites. This behavior does not depend upon the way in which Co and Al were introduced (methods i and ii). Note that the results described in the last paragraph correspond to Na-ZSM5 as starting material.

In order to study the Co–Al interaction in different environments, Co and Al were impregnated on H-ZSM5, thus favoring the presence of unexchanged Co species. These two elements were also impregnated on low-surface SiO_2, for comparison. Fig. 3 shows TPR results obtained for H-ZSM5 and SiO_2 impregnated with different Al/Co ratios. Surprisingly, for the lower Al/Co ratio (Co/Al = 0.15) only ca. 15% of the Co is reduced below 900 °C, either indicating that an important fraction of Co^{2+} ions are highly coordinated at exchange sites or that they are not accessible to hydrogen molecules due to the presence of extra-framework Al. The TPR profile of this sample shows small peaks between 200 and 300 °C, characteristic of Co oxides, and another peak at 634 °C, which is close to the value observed for Co^{2+} ions exchanged in NH_4-ZSM5 (compare with Fig. 2A).

The TPR profile of the H-ZSM5 impregnated with an Al/Co ratio of 0.3 again shows small low-temperature peaks and a more important peak at 770 °C. This value is close to that observed for the well-crystallized $CoAl_2O_4$ spinel, which shows a wide reduction zone between 700 and 900 °C. However, most of the Co species still remain unreduced.

When the Al/Co ratio increases to 0.9, Co species are almost totally reduced (96%) considering that most of them are in the form of Co^{2+} ions. The hydrogen consumption is distributed in three main signals: one small peak at 300 °C, another at 433 °C and a bigger one at 768 °C. It is clear that the lowest temperature peak corresponds to Co-oxides and the higher ones to $CoAl_2O_4$. The peak centered at 433 °C could be attributed to Co oxides interacting with $CoAl_2O_4$ crystals. In fact, it has been reported that small crystals of cobalt oxide attached to the spinel are more difficult to reduce than the single oxide, because of the interactions with the spinel [5].

Fig. 3B depicts TPR results for Co-Al impregnation in a low-surface area SiO_2. It is well known that Co/SiO_2 is completely reduced at temperatures below 400 °C [7,8]. When Co is co-impregnated with Al on the SiO_2 support, with Al/Co ratios of

Table 1
Cobalt reducibility in different environments

Samples	Al_{ad}/Co[a]	T_{calc} (°C)	H_2 consumption/Co		
			<300 °C		>490 °C
$Co_{4.9}Z$[b]	–	400	–	0.10	0.38
$Co_{3.7}Z$[c]	–	400	0.14	–	0.80
$Co_{4.9}Z$ + Al	0.5	550	–	0.10	0.94
Al-Co + NaZ	0.5	400	0.16	–	0.90
		550	–	–	1.09
Al-Co/HZ	0.15	550	0.03	–	0.10
	0.30		–	0.005	0.20
	0.90		0.05	0.11	0.80
Al-Co/SiO_2	0.15	550	0.4	–	0.32
	0.30		0.39	–	0.38
	1.5		–	0.43	0.67

[a] (Added aluminum/Co) atomic ratio.
[b] Co-exchanged on Na-ZSM5 (Si/Al = 9.6), 4.9 wt% of Co, $Co^{2+}/Al_{framework}$ = 0.57.
[c] Co-exchanged on NH_4-ZSM5 (Si/Al = 15), 3.7 wt% of Co, $Co^{2+}/Al_{framework}$ = 0.65.

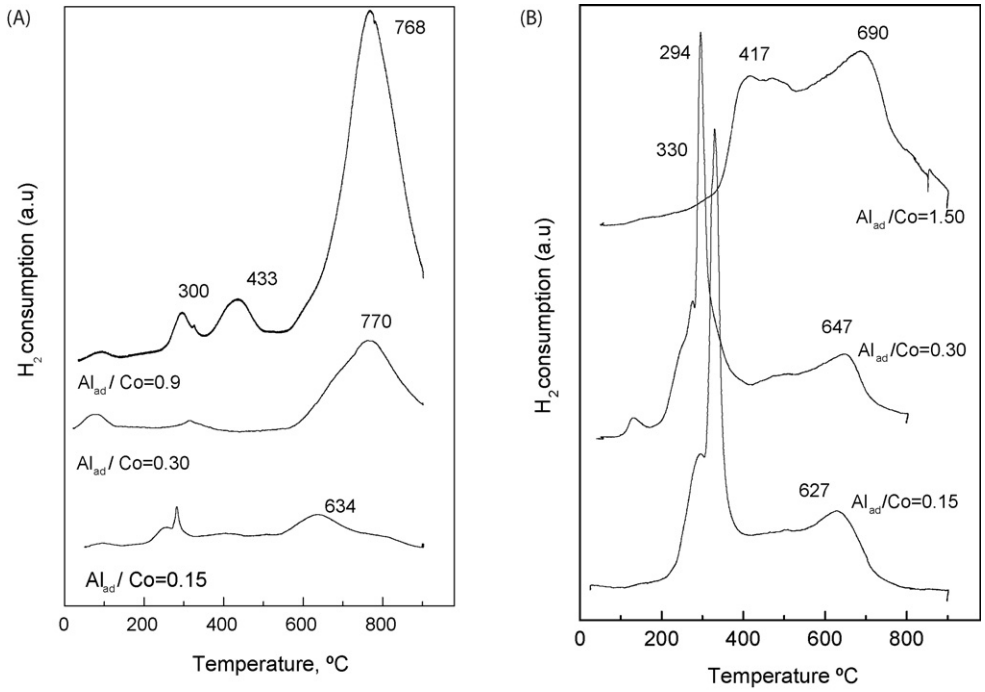

Fig. 3. (A) TPR of Al-Co-/H-ZSM5 with different Al_{ad}/Co ratios, calcined at 550 °C. (B) TPR of Al-Co/SiO_2 with different Al_{ad}/Co ratios, calcined at 550 °C.

0.15 and 0.30, sharp reduction signals are observed at 330 and 294 °C, respectively, accompanied by higher temperature peaks at 627 and 647 °C. A rather small peak insinuates around 450 °C. On the basis of what was discussed above, these signals indicate the presence of Co-oxides, $CoAl_2O_4$ spinel, and a small amount of Co-oxide interacting with the spinel. When the Al/Co ratio is increased to 1.5, the lowest temperature peak disappears, leaving those attributed to $CoAl_2O_4$ (690 °C) and Co-oxides interacting with the spinel (417 °C). If we compare Fig. 3A and B, the samples with Al/Co = 0.15 have a qualitative similar behavior with a higher extent of reduction when SiO_2 is the support. However, it is observed that for higher Al/Co ratios, the peak attributed to $CoAl_2O_4$ shifts at higher temperatures for the Co-HZSM5 sample, indicating that some interaction between the spinel and the zeolite matrix does occur.

3.3. Raman results

The LRS spectra of Co-Al impregnated on H-ZSM5 are shown in Fig. 4. These can help us to better understand the nature of the Co species. The characteristic signals of the zeolite (bands at 375 and 345 cm^{-1}) can be seen together with a strong signal at 690 cm^{-1}, which is common to both Co_3O_4 and cobalt aluminate. Note, however, that this band becomes stronger when the Al/Co ratio increases. If we compare these results with those depicted in Fig. 3A, we can relate the growth of the 690 cm^{-1} band with the increase of the higher temperature reduction peaks, thus suggesting that the signal has an important contribution from $CoAl_2O_4$ species. Moreover, the presence of a weak band in the 755–770 cm^{-1} range, which is characteristic of the aluminates, further supports this interpretation [9,10]. Note that the above-described LRS

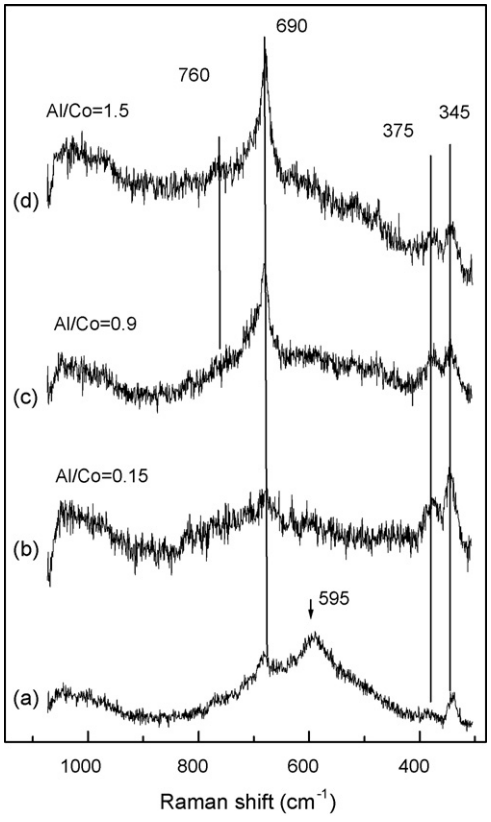

Fig. 4. Laser Raman spectra of (a) $Co_{4.9}Z$ plus $Al(NO_3)_3$; (b–d) Al-Co-/H-ZSM5 with different Al_{ad}/Co ratios, calcined at 550 °C. Bands of reference compounds: 753, 690, 619, 519, 480, 412, 198 cm^{-1}, and 690, 619, 519, 480 and 198 cm^{-1} for Co_3O_4 [9,10].

spectra correspond to Co impregnated on H-ZSM5 by the incipient wetness method, in order to favor the presence of unexchanged-Co species together with extra-lattice Al. In Fig. 4, an LRS spectrum of Co-exchanged sample plus $Al(NO_3)_3$ added in the slurry is shown for comparison. It can be seen that the band at 690 cm^{-1} is weaker, and a stronger band appears at 595 cm^{-1}, which can be assigned to highly dispersed Co_xO_y [6]. Thus, in the exchanged sample, aluminate species are less developed than in the impregnated ones. These results are in agreement with the TPR data in Fig. 2B, which show the main reduction signal in the 490–510 °C temperature range and cannot be assigned to a well-developed $CoAl_2O_4$ phase.

The LRS spectra of SiO_2 supported Co and Al, similarly to the impregnated Co-HZSM5, show a dominant peak at 690 cm^{-1} together with less intense bands at 753, 619 and 412 cm^{-1} (Fig. 5). Even though the peak at 755 cm^{-1} seems not to be completely defined in the Raman spectra of Fig. 5. The formation of cobalt aluminate is supported by the appearance of a second reduction peak at higher temperatures than 600 °C, which increases with the increase of the aggregated aluminate percentage and by the modified Auger parameter of $Al_{(KLL)}$ (1461.8 eV), shown in Table 2, which corresponds to Al at octahedral positions.

In sum, TPR together with LRS spectra suggest that a non-fully developed mixed oxide, probably a non-stoichiometric spinel $Co_{1+y}Al_{2-x}O_4$ plus small Co_xO_y particles are present in the Co-exchanged sample when $Al(NO_3)_3$ is added to the slurry. These species can partially evolve to Co_3O_4 and $CoAl_2O_4$ under

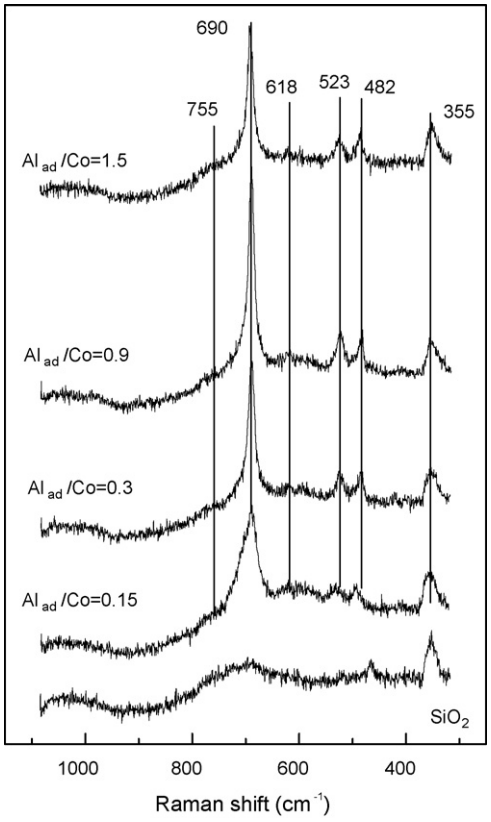

Fig. 5. Laser Raman spectra of Al-Co/SiO_2 with different Al_{ad}/Co ratios, calcined at 550 °C.

Table 2
XPS data obtained with Al-Co/HZ and Al-Co/SiO_2

Sample	Al_{ad}/Co	Binding energies, (eV)			Co/Si
		$Co2p_{3/2}$	Al2p	α'_{KLL} [a]	
Al-Co/HZ	0.15	782.1(53) [b] 779.8(47) [b]	74.5	1460.8	0.065
	0.30	780.0(80) [b] 779.8(20) [b]	74.4	1460.9	0.056
	0.90	782.0	74.5	1460.3	0.097
	1.5	782.1	74.5	1460.4	0.067
Al-Co/SiO_2	0.15	780.7	74.5	1460.8	0.536
	0.30	781.0	74.5	1461.8	0.501
	0.9	780.1	74.5	1461.8	0.228

[a] Modified Al Auger parameter, $\alpha'_{KLL} = EE\,Al2p + EK\,Al_{KLL}$.
[b] Species percentage referred to total cobalt.

NO_x SCR in a wet atmosphere [5]. In the case of impregnated samples, Co_3O_4 and $CoAl_2O_4$ are present after calcination.

3.4. XPS measurements

XPS data were obtained with the samples prepared by impregnation. The binding energies of Al2p (Table 2) and Al2s do not change in the seven solids studied, i.e. Al2p = 74.5 eV, Al2s 119.0–119.3 eV. The Si2p BE was 103.4 for the silica supported samples and 102.7–103.0 eV for those prepared on H-ZSM5.

The Auger parameter, α', yielded more interesting information. All the H-ZSM5 samples showed values between 1460.3 and 1460.9 eV (Table 2), which were assigned to the tetrahedral Al of the zeolite structure. However, the same parameter shifted to 1461.8 eV when SiO_2 was used as a support for Al/Co ratios of 0.3 and 0.9. This α' value was assigned to octahedral Al centers typical of the aluminate structure [11].

The BEs of $Co2p_{3/2}$ reported in Table 2 vary between 779.8 and 782.1 eV. The BEs between 779.5 and 780.5 eV are characteristic of cobalt oxides, particularly Co_3O_4 [12,13]. Co^{2+} ions sitting at exchange positions in ZSM5 show a signal centered around 782 eV [14,15].

For $Co2p_{3/2}$ in $CoAl_2O_4$, the literature reports values between 781.7 and 782 eV impossible to distinguish from Co^{2+} at exchange positions [12,16]. However, by analyzing the TPR results of the impregnated samples, Fig. 3A (Al-Co-/H-ZSM5) and B (Al-Co/SiO_2) and those corresponding to their LRS spectra (Figs. 4 and 5, respectively) we can differentiate the surface cobalt species (2^+). In the case of the impregnated ZSM5, the oxides present at low Al_{ad}/Co ratio disappear when more $Al(NO_3)_3$ is added due to the formation of the aluminate. In the case of SiO_2, the Al/Co ratio is not enough to form exclusively the aluminates, thus, the reported BEs could be the result of the simultaneous presence of cobalt oxides (e.g. Co_3O_4) and cobalt aluminates.

3.5. XRD data

Due to the similar diffractograms of the spinel structure of Co_3O_4, $CoAl_2O_4$ and Co_2AlO_4, it is very hard to distinguish

among these compounds based upon this technique. Furthermore, in the case of ZSM5, there are several reflections that overlap with those belonging to the cobalt compounds. When SiO_2 is the support, the main spinel reflections are seen at 2θ: 31.25°, 36.84°, 44.81°, 59.29°, and 65.25°. Thus, the XRD data are consistent with the information obtained with the other instrumental techniques.

4. Conclusions

The identification of the cobalt mixed oxides formed when the washcoating suspension contained both Co-ZSM5 and $Al(NO_3)_3$ was achieved through a systematic study of different related systems such as Al + Co impregnated ZSM5 and SiO_2.

When Al^{3+} and Co^{2+} are present in the aqueous suspension containing ZSM5, the strong interaction between these ions impair the exchange of Co^{2+} and originates a new mixed oxide of the $Co_{1+y}Al_{2-x}O_4$ type after calcination at 550 °C. This oxide is inactive for the CH_4-SCR of NO_x (Fig. 1).

The Raman spectra of the impregnated samples showed the band at 755–770 cm^{-1} pertaining to $CoAl_2O_4$ plus the 690, 619, 523 and 482 cm^{-1} that are common also to the Co_3O_4 spinel (Figs. 4 and 5). Furthermore, the modified Al Auger parameter identified the presence of octahedral aluminum, characteristic of the aluminate in co-impregnated SiO_2 samples (Table 2).

Acknowledgments

The authors wish to acknowledge the financial support received from ANPCyT, CONICET and UNL. Thanks are also given to Elsa Grimaldi for the English language editing.

References

[1] T.A. Nijhuis, A.E. Beers, T. Vergunst, I. Hoek, F. Kapteijn, J.A. Moulijn, Catal. Rev. 43 (4) (2001) 345.
[2] P. Avila, M. Montes, E. Miro, Chem. Eng. J. 109 (2005) 11.
[3] J.M. Zamaro, M.A. Ulla, E.E. Miró, Chem. Eng. J. 106 (2005) 25.
[4] A. Boix, J.M. Zamaro, E.A. Lombardo, E.E. Miró, Appl. Catal. B: Environ. 46 (2003) 121.
[5] A.V. Boix, E.E. Miró, E.A. Lombardo, M.A. Bañares, R. Mariscal, J.L.G. Fierro, Appl. Catal. A 276 (2004) 197.
[6] A.V. Boix, E.E. Miró, E.A. Lombardo, M.A. Bañares, R. Mariscal, J.L.G. Fierro, J. Catal. 217 (2003) 186.
[7] P. Arnoldy, J.A. Moulijn, J. Catal. 93 (1985) 38.
[8] R. Brown, M.E. Cooper, D.A. Whan, Appl. Catal. 3 (1982) 177.
[9] H. Ohtsuka, T. Tabata, O. Okada, L.M.F. Sabino, G. Bellussi, Catal. Lett. 44 (1997) 265.
[10] B. Jongsomjit, J. Goodwin, Catal. Today 77 (2002) 191.
[11] M.J. Remy, M.J. Genet, G. Poncelet, P.F. Lardinois, P.P. Notté, J. Phys. Chem. 96 (1992) 2614.
[12] Z. Zsoldos, L. Guczi, J. Phys. Chem. 96 (1992) 9393.
[13] R.L. Chin, D.M. Hercules, J. Phys. Chem. 86 (1982) 360.
[14] A.V. Boix, J.L.G. Fierro, Surf. Interface Anal. 27 (1999) 1107.
[15] J.M. Stencel, V.U.S. Rao, J.R. Diehl, K.H. Rhee, A.G. Dhere, R. De Angels, J. Catal. 84 (1983) 109.
[16] P. Thormahlen, E. Fridell, N. Cruise, M. Skolundh, A. Palmqvist, Appl. Catal. B 31 (2001) 1.